6 Diffusion Tensor Imaging and Functional Magnetic Resonance in Brain Tumor Imaging

Ömer Kitiş and Sevcan Türk

6.1 Introduction

The main goal of brain tumor surgery is to remove the mass as completely as possible while ensuring minimal neurological deficits. For this reason, prior to surgery, neurosurgeons must be able to recognize associations between the tumor and specific eloquent cortical areas (such as the motor-sensory cortex, speech center, visual cortex, and dominant hemisphere) as well as important white matter (WM) tracts (such as the corticospinal tract and arcuate fasciculus) (Table 6.1). Functional magnetic resonance imaging (fMRI) and diffusion tensor imaging (DTI) can provide sufficient data in this respect, and these modalities are preferable to other modalities of assessment. fMRI enables the noninvasive localization and lateralization of specific areas of brain function via the measurement of local hemodynamic changes coupled with neuronal activation. On the other hand, DTI also presents valuable imaging data via the estimation of major WM bundles. The advantages of both fMRI and DTI are their noninvasiveness, lack of ionizing radiation, data reproducibility, and practicality due to the broad availability of MRI scanners [1–8].

Table 6.1 The main goals of neuroimaging for presurgical planning

• Demonstrating the anatomic relationship between the area of surgery and the eloquent cortex as well as major WM fibers
• Determining the relationship between the brain tumor and the eloquent cortex as well as major WM fibers
• Identifying the dominant hemisphere
• Investigating the neuronal plasticity of specific brain functions

6.2 DTI

Because the surgical injury of WM tracts can result in significant permanent neurologic deficits, neurosurgeons generally employ tractography in routine preoperative planning. The most common identification method for WM tracts is DTI, which measures the direction of the diffusion of water molecules in order to locate the axis of these tracts. DTI presumes that axonal membranes and myelin directionally restrict the diffusion of water. In brain tissue, most water molecules move parallel to fiber tracts, which results in anisotropic diffusion in regions of tightly packed WM bundles. Conversely, these molecules disperse equally in all directions (isotropic) in cerebrospinal fluid (CSF) and gray matter. In DTI, magnetic gradients are applied in at least six directions. The diffusion tensor is calculated via a mathematical model that estimates the direction of maximum diffusivity of water molecules for each voxel, which corresponds to the main axis of

Ö. Kitiş (✉) · S. Türk
School of Medicine, Ege University, Bornova, Izmir, Turkey

Y. Özsunar, U. Şenol (eds.), *Atlas of Clinical Cases on Brain Tumor Imaging*,
https://doi.org/10.1007/978-3-030-23273-3_6

WM tracts in the respective location. DTI-based tractography—a three-dimensional mapping algorithm of WM tracts obtained by diffusion-weighted imaging (DWI)—is the most common neuroimaging technique used to reveal WM structure (Fig. 6.1). From DWI signals, it is possible to generate an anisotropic map showing WM tracts, their orientations, and their relation to possible brain lesions. DTI can successfully determine major WM tracts, including the corticospinal, corticobulbar, and corticopontine tracts; arcuate fasciculus (AF), uncinate fasciculus, superior and inferior occipitofrontal fasciculi, and occipitotemporal fasciculus; optic radiation; corpus callosum; cingulum; and anterior commissure. The corticospinal tract (CST) and AF are the most important WM pathways most commonly investigated by DTI-based tractography because of their importance to motor functions and language, respectively [1, 3, 4, 7].

DTI is a relatively stable method since it is neither user-dependent nor task-based. However, one of its disadvantages is its relatively long acquisition time, meaning that movement artifacts can affect image quality. Although DTI acquisition time depends on many parameters such as the number of gradient directions, imaging matrix, slice thickness, and number of acquisition, it can nevertheless be obtained at acceptable image quality within 3–4 min on a 3 T MRI scanner.

6.2.1 Alteration of DTI Patterns in WM Tracts by Tumors

The major effects of brain tumors on WM tracts include deviation, infiltration, and disruption (Figs. 6.2 and 6.3). Jellison et al. have described four major patterns in affected WM tracts categorized on the basis of anisotropy and fiber direction

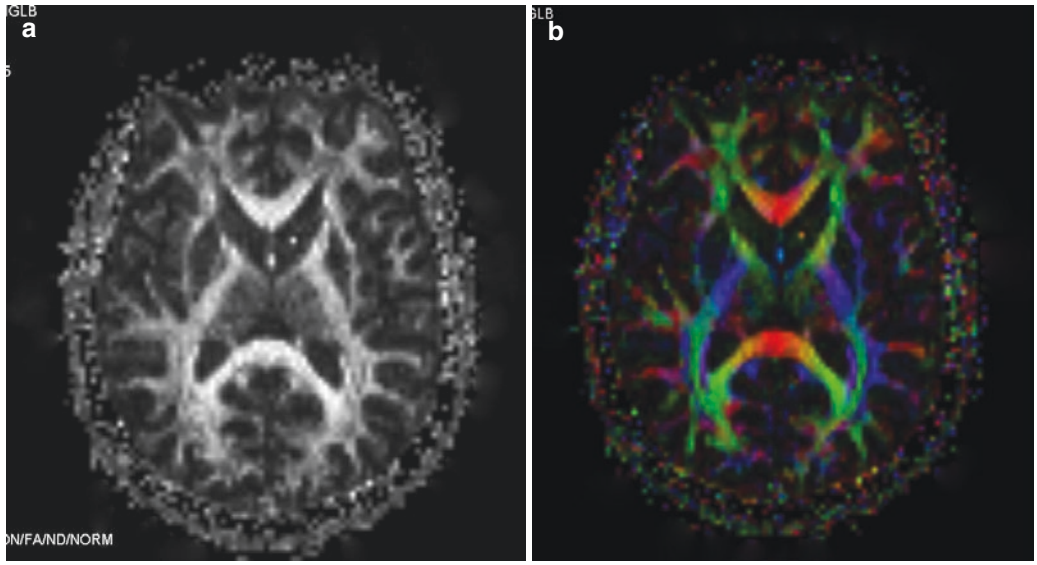

Fig. 6.1 DTI data set from a normal control case. (**a**) Gray-scale FA map showing the degree of anisotropy. Brighter areas (higher FA values) contain more anisotropy than darker areas (lower FA). (**b**) Color-coded FA map providing information regarding diffusion direction by using the largest eigenvalue within the voxel. The color red is used to indicate diffusion along the left/right axis, green for diffusion along the anterior/posterior axis, and blue for diffusion along the inferior/superior axis. (**c**) 3D fusion images including a color-coded FA map superimposed on 3D anatomical T1-weighted (MP-RAGE sequence) images. (**d**) DTI-based fiber tracking. The left CST (yellow arrows) has been reconstructed from DTI data by choosing a seed point at the level of cerebral peduncle. (**e**) 3D fiber tractography of the right AF (yellow arrows)

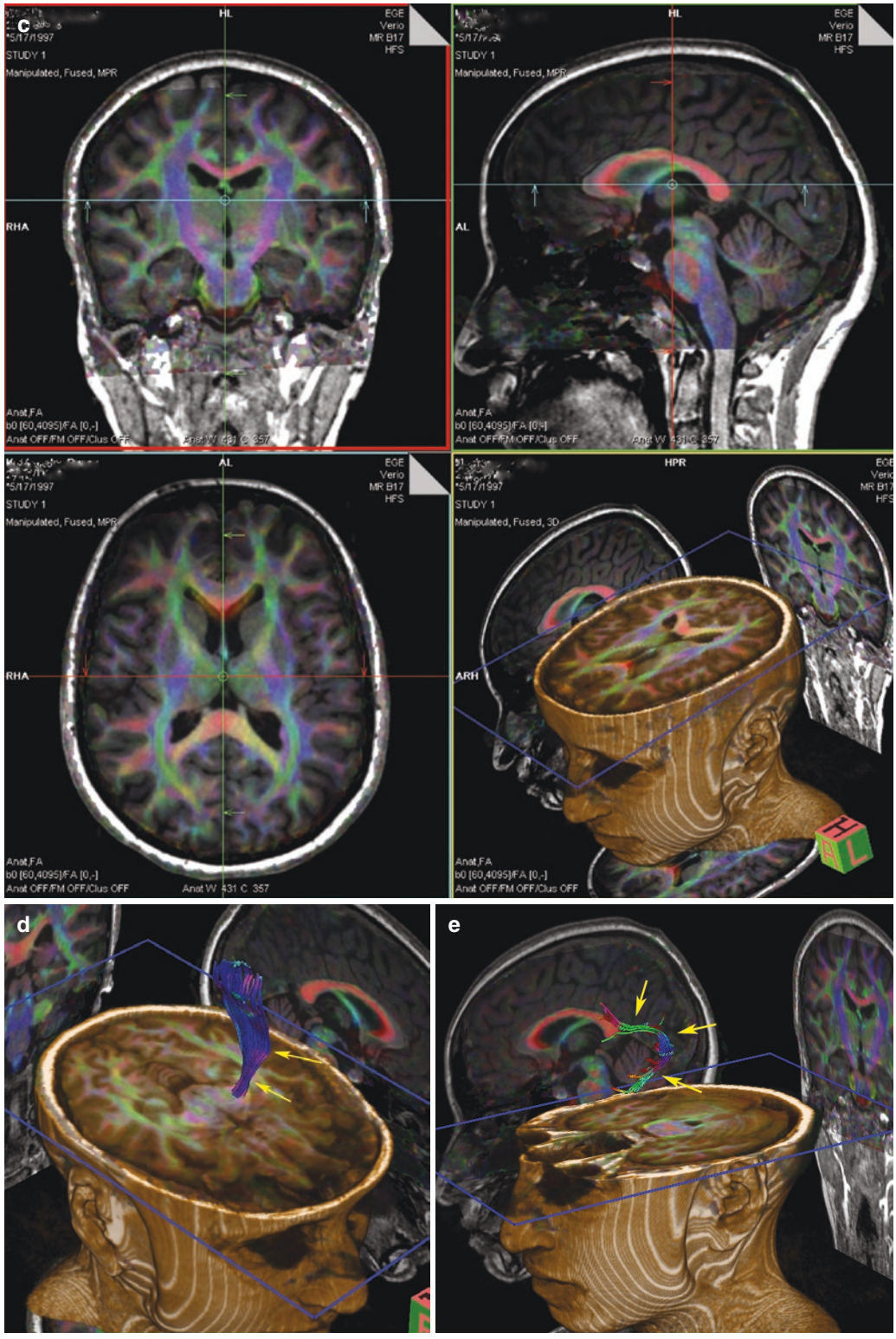

Fig. 6.1 (continued)

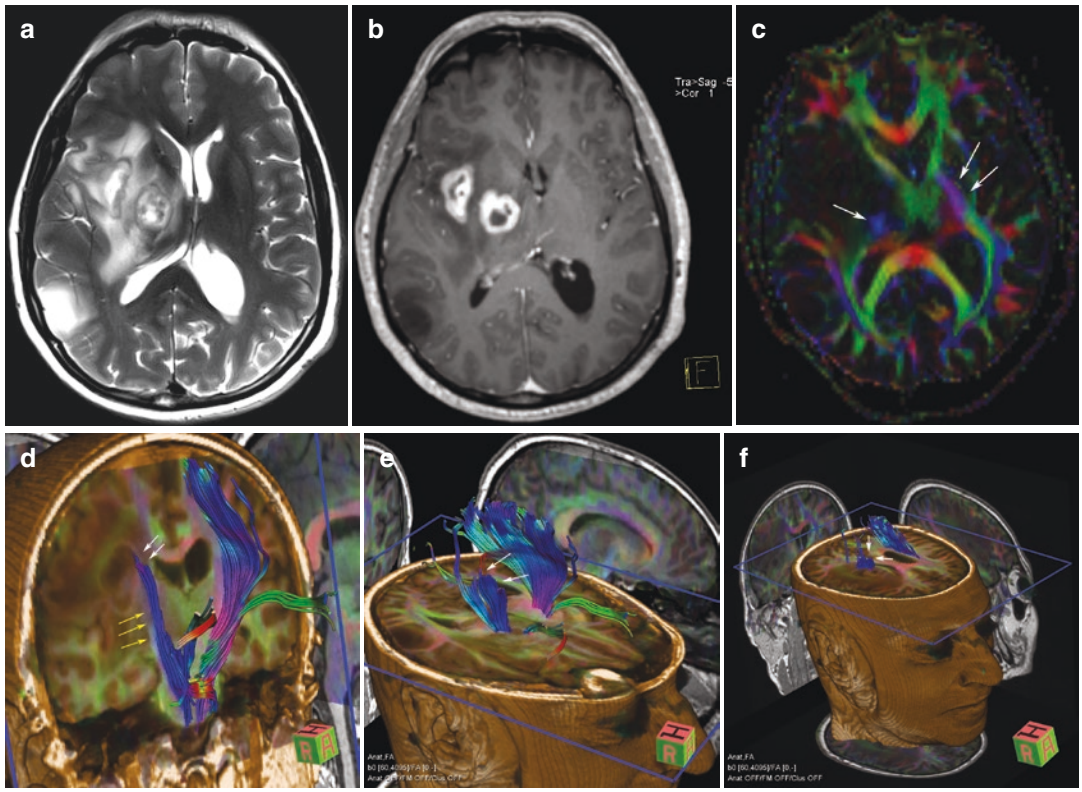

Fig. 6.2 A patient with multicentric glioblastoma in the right hemisphere. This patient complained of left hemiparesis, which had been caused by the infiltration of the tumor in the right posterior capsula interna. (**a**, **b**) Indicate right multicentric contrast-enhancing masses infiltrating the right basal ganglia and occipitotemporal cortex. (**c**) Involves a color-coded FA map which reveals the marked tumoral disruption of anisotropy in the infiltrated parenchyma. On the left side, normal CST (white arrows) is represented by magenta. However, the right CST (white arrow) appears in blue, secondary to the disruption of anisotropy. (**d**–**f**) Contain DTI tractography images, which show the displacement (yellow arrows) and interruption (white arrows) of the CST bundles

or orientation [4]. Pattern 1 involves normal or only slightly decreased fractional anisotropy (FA) with abnormal location and/or direction resulting from the mass effect of the tumor. This means that WM tracts are intact and can be preserved during surgery. Pattern 2 is typified by decreased FA with normal location and direction. This pattern is frequently observed in the vasogenic edema surrounding tumors such as metastases or meningiomas. Pattern 3 entails substantially decreased FA with abnormal hues on directional color maps. This pattern can be found in a small number of infiltrating gliomas. Finally, Pattern 4 involves isotropic (or near-isotropic) diffusion such that the tract cannot be identified on directional color maps. This pattern is observed when a part of a tract is completely disrupted by a tumor.

In addition to fiber tractography, DTI also enables the measurement of various parameters—such as the shape, magnitude, and degree of diffusion anisotropy—which may be used to differentiate brain tumors. DTI metrics such as mean diffusivity (MD), linear anisotropy coefficient (CL), planar anisotropy coefficient (CP), spherical anisotropy coefficient (CS), and FA can be used individually or in combination for brain tumor classification. However, these metrics play a limited role in the differentiation of brain tumors. Relatively newer and more advanced diffusion techniques such as diffusion kurtosis imaging (DKI) and diffusion spectrum imaging (DSI) may provide additional information [3] in this regard.

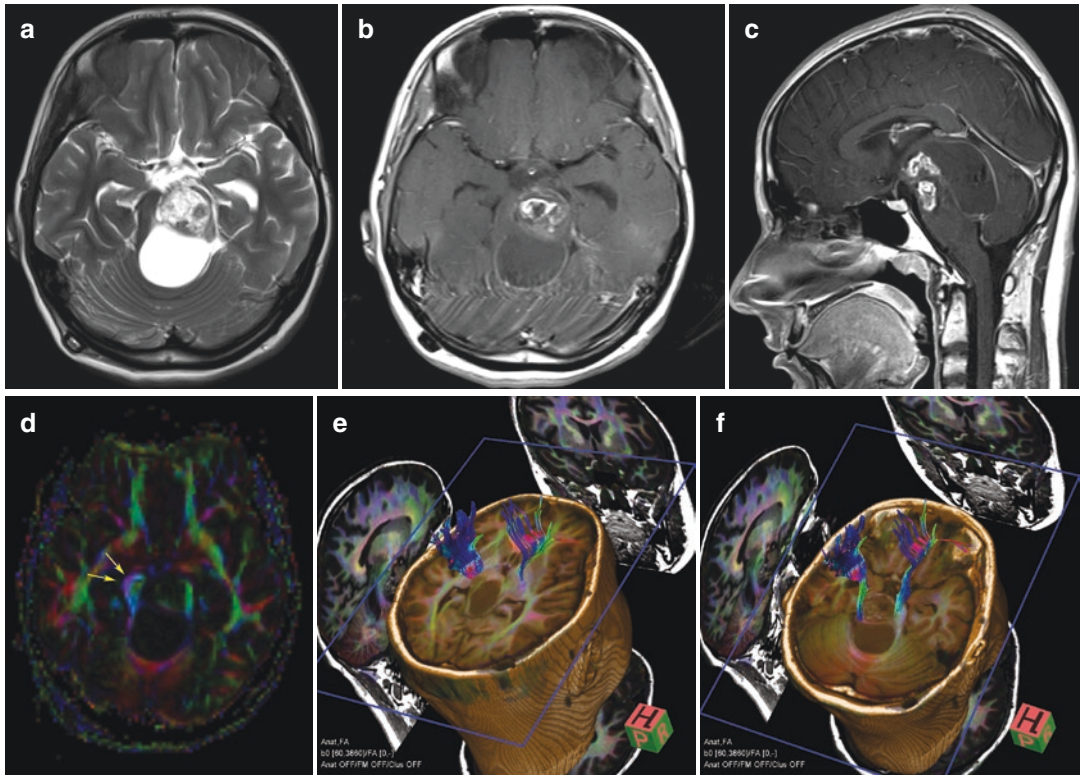

Fig. 6.3 Sixteen-year-old girl with brain stem glioma (pilocytic astrocytoma). A large mass containing a posterior cystic component and contrast-enhancing solid portions was observed in the brainstem (**a**–**c**) of this patient, the cyst had obliterated the fourth ventricle. A neurosurgeon advised an examination of the CST in order to assess the anatomic relation of the tumor to the CST inside the brainstem. A color-coded FA map (**d**) displays the right CST (yellow arrows) in magenta, but this was not visible on the left due to compression and a decrease in anisotropy. DTI tractography (**e**, **f**) revealed the exact bilateral location of CST fibers and anatomic relation to the tumor. In this case, tractography was enabled to plan an appropriate preoperative approach and safe surgical trajectory to neurosurgeon

6.3 fMRI

Blood-oxygen-level-dependent fMRI (BOLD fMRI) is a noninvasive brain mapping method that enables the indirect measurement of neuronal activity as a consequence of neurovascular coupling. During neuronal activation, local cerebral blood flow (CBF) increases with a consequent increase in oxyhemoglobin and decrease in deoxyhemoglobin concentration in venules. These molecular changes cause the transient distortion of local magnetic field homogeneity, and this effect can be detected by T2* gradient echo sequences. While oxyhemoglobin is diamagnetic, deoxyhemoglobin is a paramagnetic molecule. Since the increase in oxyhemoglobin is greater than the decrease in deoxyhemoglobin, the diamagnetic effect dominates local signal changes. This phenomenon results in the increase of transient T2* signals (BOLD signals) within the activated cerebral cortex. Since the magnitude of the BOLD signal is only around 2–4% at 1.5 T and 4–8% at 3 T, it is necessary to create multiple resting and activation conditions in order to detect activation-related signals and exclude noise [2].

fMRI examinations are performed using event-related and block-design paradigms, which consist of sensorimotor, cognitive, and visual tasks. In routine clinical practice, block-design fMRI is widely used due to its high

signal detection capability, easier design and implementation, and better patient participation. Neurosurgeons commonly advise patients with brain tumors to seek preoperative evaluation of the motor cortex and language lateralization in order to determine the exact anatomic location of the tumor and its association with eloquent brain regions.

6.3.1 Paradigms for the Primary Motor Cortex

Common paradigms used for the primary motor area are relatively easy tasks such as finger-tapping and tongue- and foot movement (Figs. 6.4 and 6.5). In most cases, patients can perform these tasks successfully, and these

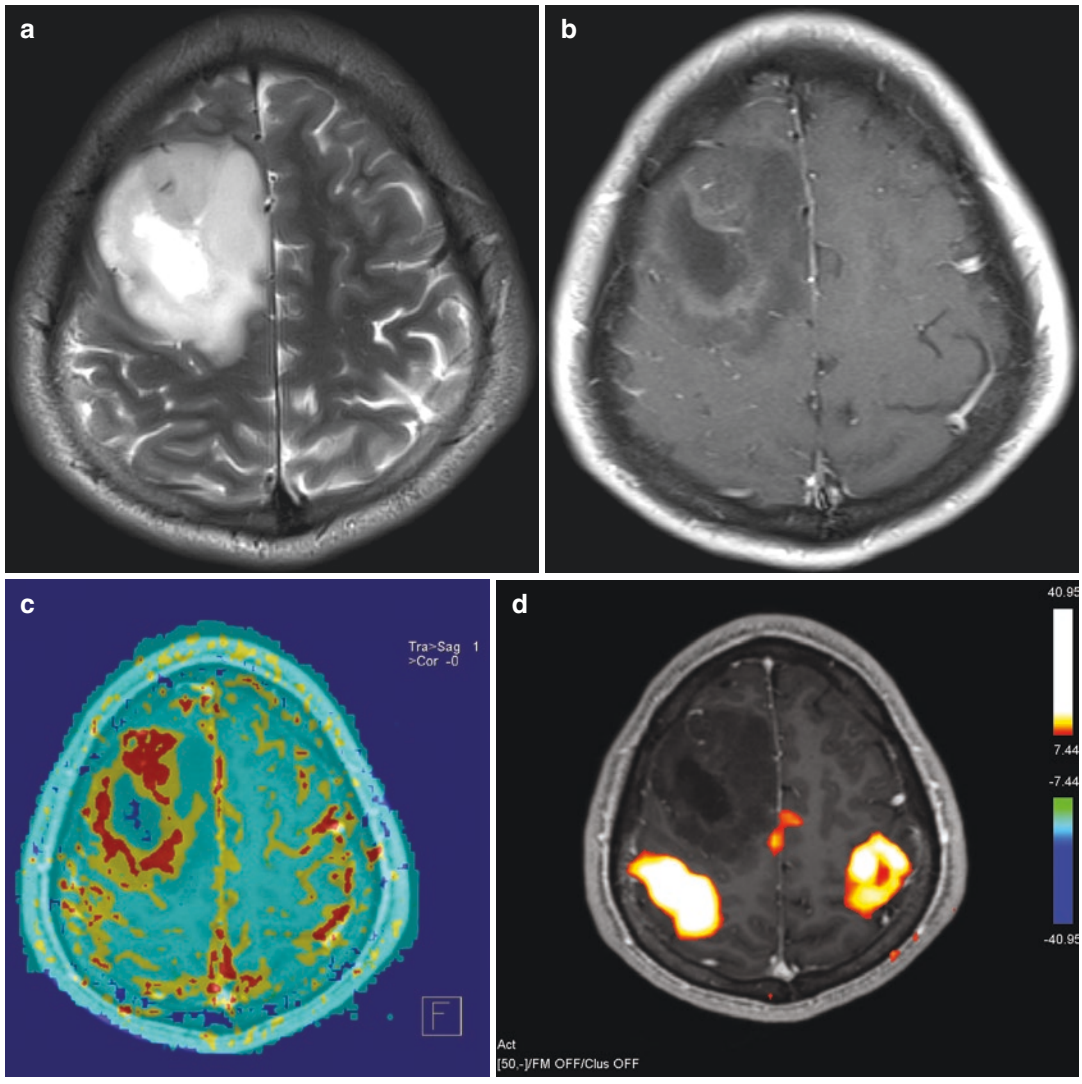

Fig. 6.4 These images indicate a right frontal mass possessing heterogeneity and moderate enhancement (**a**, **b**). The tumor displayed high perfusion (increased cerebral blood volume) on a relative cerebral blood volume (r-CBV) map (**c**, perfusion MRI), which is consistent with high grade. Since the tumor was located in the anterior Rolandic area, motor fMRI (finger-tapping) was conducted to identify the relation of the tumor to the eloquent motor cortex. fMRI activation maps overlaid with T2 and 3D T1-weighted images (**d**–**h**) reveal that there was no invasion in the motor-sensory cortex. Normal parenchyma can be seen between the tumor and adjacent precentral gyrus. On sagittal images (**f**, **h**), the superior part of the tumor can be seen in close proximity to the activation (white arrows), but this is possibly due to an exaggeration of the activation caused by a large cortical vein (venous effect) (yellow arrows). After surgery, the mass was diagnosed as an anaplastic astrocytoma, pathologically

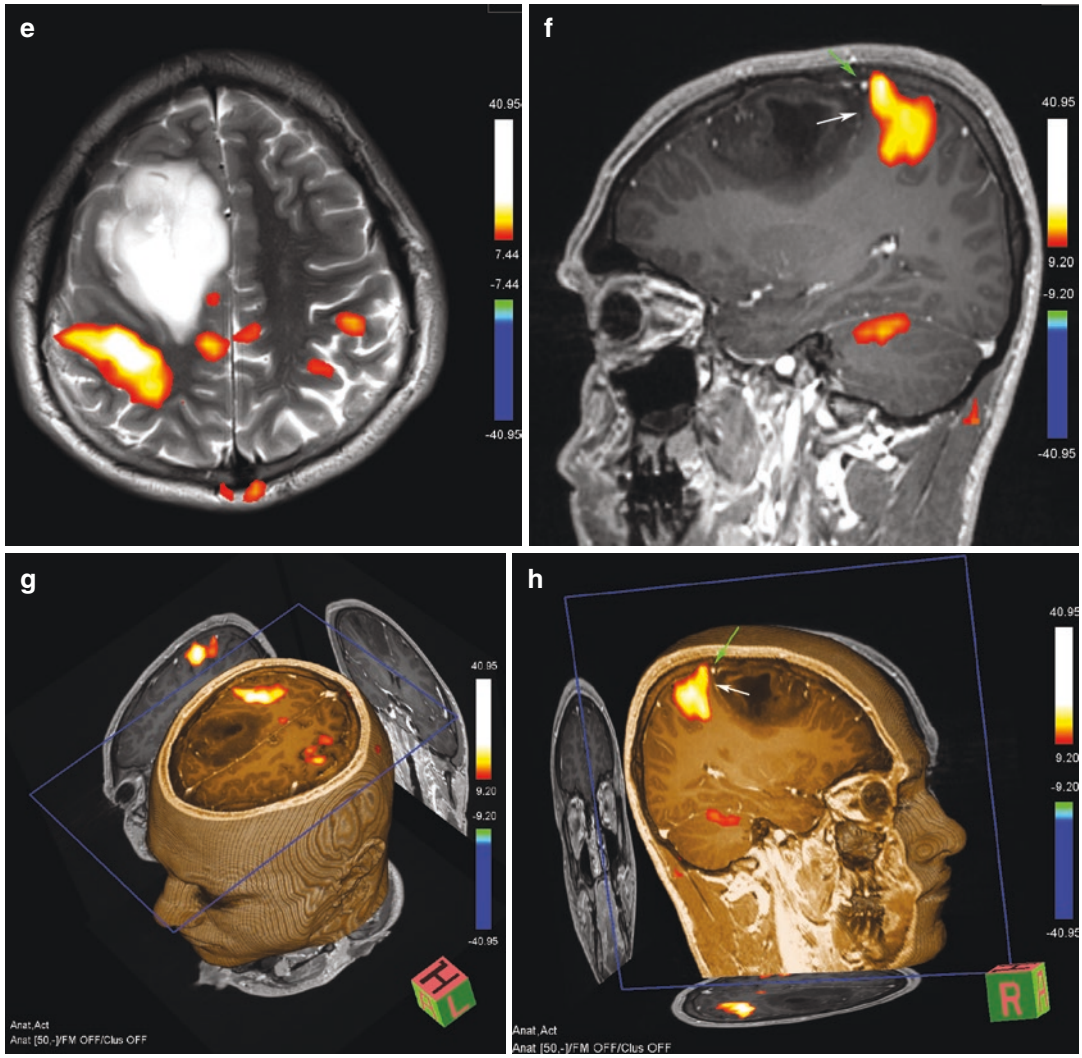

Fig. 6.4 (continued)

paradigms provide sufficient signal, especially at high-field strength.

6.3.2 Paradigms for Language Lateralization

The three main types of paradigms utilized for language lateralization are expressive, receptive, and semantic. Expressive paradigms are designed to demonstrate activation mainly in speech-production areas. The most commonly used expressive paradigms employed in fMRI for presurgical mapping are silent word generation, silent verb generation, and simple object naming (Figs. 6.5 and 6.6).

6.3.3 Statistical Analyses and the Creation of fMRI Maps

Following image acquisition and preprocessing, it is necessary to determine which voxels are of task-related activation. The most commonly used statistical method is the general linear model (GLM), which employs regression

analysis. The GLM includes modeling of both paradigm timing and expected hemodynamic response function (HRF), and the obtained model is fit to the acquired data at each voxel. Thus, the voxels with statistical significance can be displayed on a map superimposed on the anatomical image. In clinical settings, radiologists can change the thresholds of statistical significance (*t*-test, *z*-score, and *p*-value) in order to demonstrate appropriate activation and exclude noise or weak voxels.

fMRI can be processed on scanners during the performance of a paradigm (real-time processing), which is valuable in determining whether or not the task being performed is sufficient. Most clinical MRI centers contain hardware and software

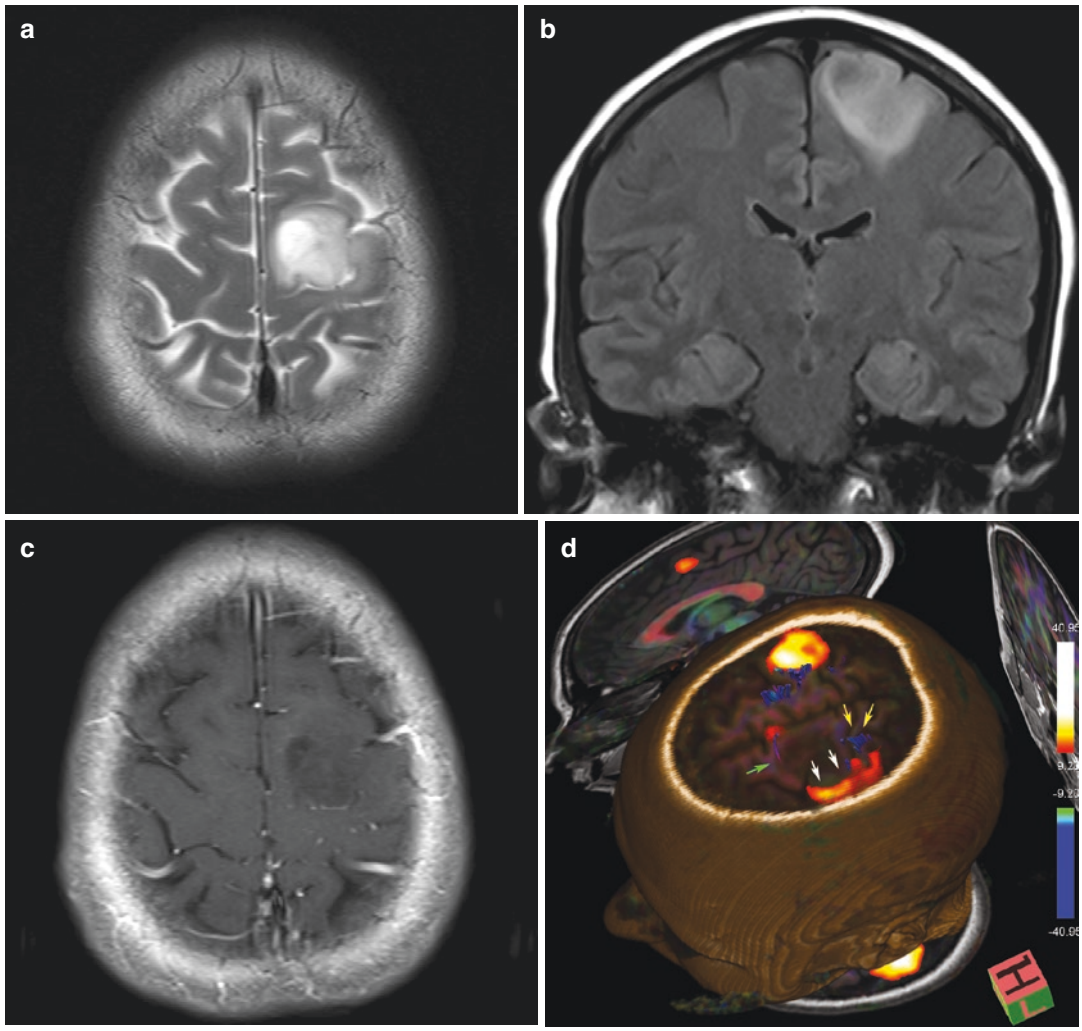

Fig. 6.5 Low-grade glioma (LGG) located in the left Rolandic region. The lesion was hyperintense on T2-weighted (**a**) and FLAIR (**b**) images and did not enhance with contrast (**c**). Both fMRI (motor-sensory activation by finger-tapping) and DTI examinations were performed and evaluated together at the preoperative stage. 3D fusion images (**d**–**f**) were formed by superimposing fMRI, DTI, and anatomical data at the workstation. Both activated motor cortex (red areas) and terminal CST fibers (blue bundles) could be seen on the 3D fusion images. The LGG had displaced the motor cortex (white arrows) laterally. The ventral CST fibers, however, seem to have been slightly separated (green arrows), and most of the CST fibers (yellow arrows) had been displaced posteriorly by the tumor

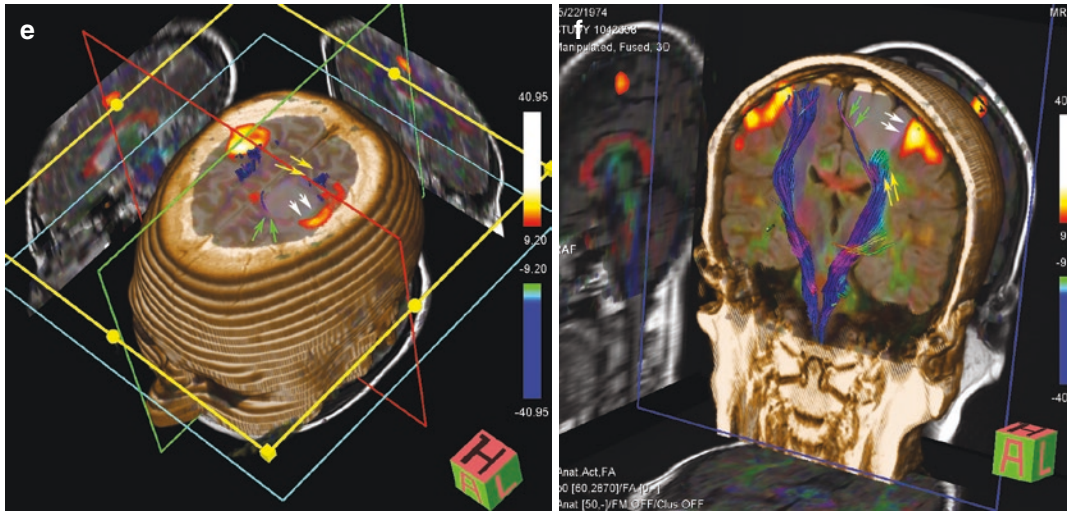

Fig. 6.5 (continued)

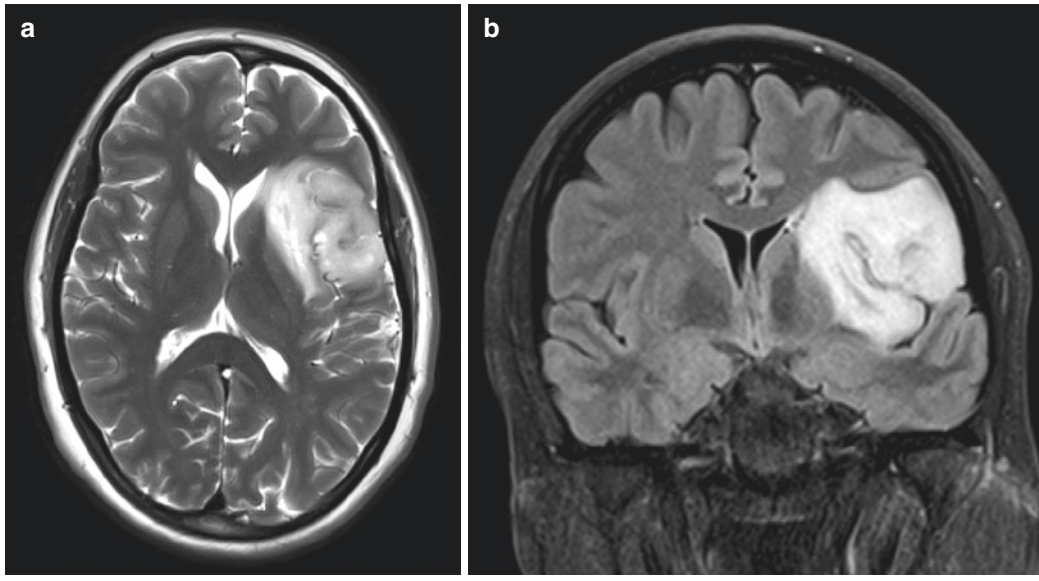

Fig. 6.6 Right-handed 48-year-old female patient with oligodendroglioma. T2-weighted and FLAIR images (**a**, **b**) show a mass in the left frontal operculum. Since the patient was right-handed, the left hemispheric dominancy possibility was 98%. Thus, it was suspected that this tumor may have infiltrated eloquent speech areas because of its location. Motor-sensory BOLD maps overlaid to T2-weighted images (**c**) reveal no close relationship between the motor-sensory cortex and the tumor, as was expected. In the second session of the fMRI exam, verb generation and word generation tasks were utilized to activate the dominant hemisphere and speech centers. The activation maps (**d**) obtained from the performance of a silent verb generation paradigm fused with T2 FLAIR structural images indicate that areas of neuronal activation were present at the superior and superoposterior margins of the lesion. DTI tractography images indicate that rostral AF was located at the posterior margin of the tumor (**e**). The DTI-fMRI fusion image (**f**) displays the anatomical relationship between the tumor with AF and language-related neuronal activation areas

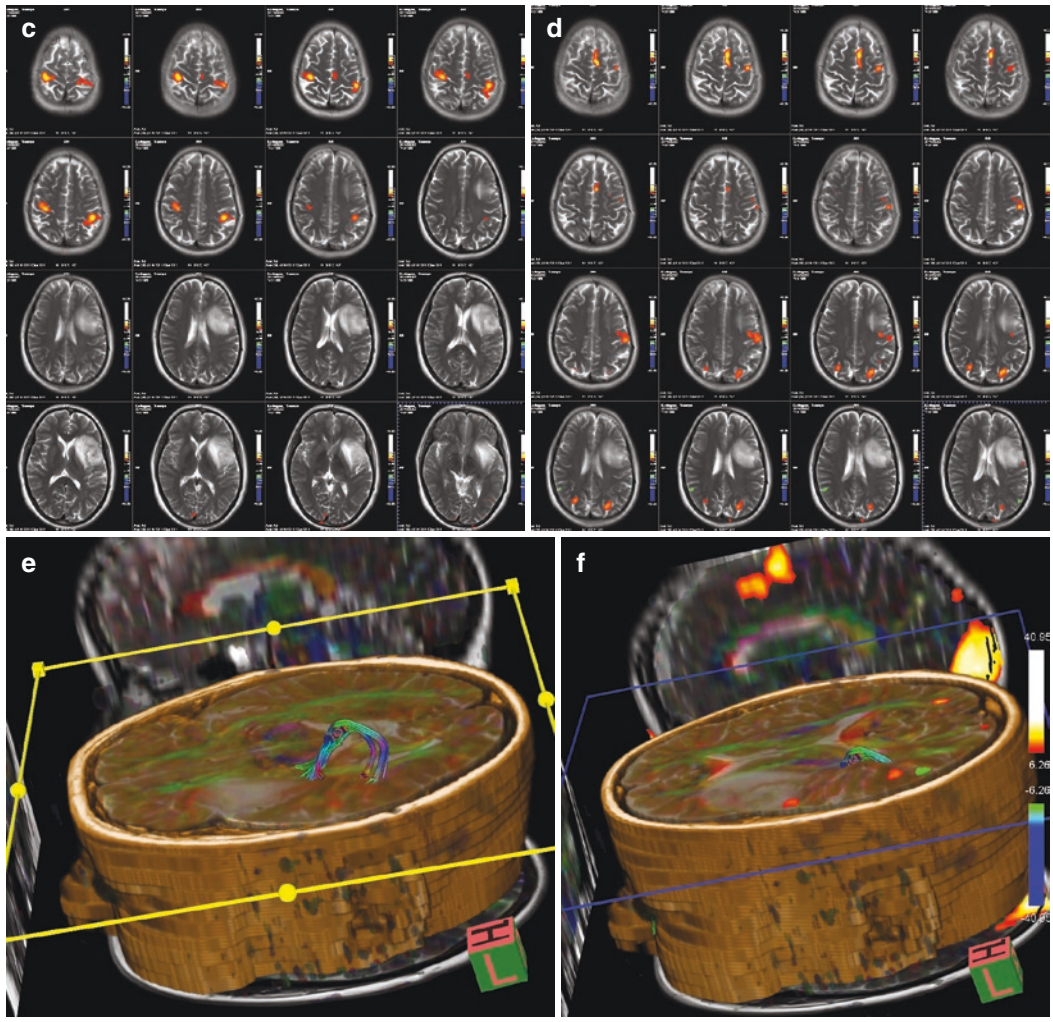

Fig. 6.6 (continued)

that allow the use of techniques such as motion correction, time correction, filtering, and anatomic co-registration in order to optimize the quality of the examination.

The paradigms used in motor-sensory fMRI are relatively simple, and the signal obtained from the task is strong, as well. Therefore, outlining the eloquent cortex by the use of a sensorimotor fMRI is a reliable method. In studies comparing electrocortical stimulation mapping (ESM) to sensorimotor fMRI, the accuracy of fMRI has been proven to be over 90% and the rate reaches 100% with the use of a 3 T scanner [8].

When compared with the Wada test and other invasive mapping techniques such as ESM, fMRI of language processing has proven 90% validity and higher. Thus, fMRI is widely utilized as the initial test of choice for determining language lateralization in preoperative patients. However, the use of language fMRI for identifying eloquent language areas has been proven as less accurate than that of sensorimotor fMRI. Therefore, the preoperative application of multiple language paradigms is essential for evaluating multiple language regions and recommended for enhancing sensitivity [8].

References

1. Mormina E, Longo M, Arrigo A, Alafaci C, Tomasello F, Calamuneri A, Marino S, Gaeta M, Vinci SL, Granata F. MRI tractography of corticospinal tract and arcuate fasciculus in high-grade gliomas performed by constrained spherical deconvolution: qualitative and quantitative analysis. AJNR Am J Neuroradiol. 2015;36:1853–8.
2. Stippich C. Clinical functional MRI presurgical functional neuroimaging. 2nd ed. Berlin: Springer; 2015.
3. Van Hecke W, Emsell L, Sunaert S. Diffusion tensor imaging: a practical handbook. New York: Springer; 2016.
4. Jellison BJ, Field AS, Medow J, Lazar M, Shariar Salamat M, Alexander AL. Diffusion tensor imaging of cerebral white matter: a pictorial review of physics, fiber tract anatomy, and tumor imaging patterns. Am J Neuroradiol. 2004;25(3):356–69.
5. Pillai JJ. Functional brain tumor imaging. New York: Springer; 2014.
6. Silva MA, See AP, Essayed WI, Golby AJ, Tie Y. Challenges and techniques for presurgical brain mapping with functional MRI. Neuroimage Clin. 2018;17:794–803.
7. Soni N, Mehrotra A, Behari S, Kumar S, Gupta N. Diffusion-tensor Imaging and tractography application in pre-operative planning of intra-axial brain lesions. Cureus. 2017;9(10):e1739.
8. Wang LL, Leach JL, Breneman JC, McPherson CM, Gaskill-Shipley MF. Critical role of imaging in the neurosurgical and radiotherapeutic management of brain tumors. Radiographics. 2014;34(3):702–21.